

The Frequency of Polarized Broad Emission Lines in Type 2 Seyfert Galaxies

Edward C. Moran^{1,2}, Aaron J. Barth³, Laura E. Kay^{4,5}, and Alexei V. Filippenko²

ABSTRACT

We have discovered polarized broad emission lines in five type 2 Seyfert galaxies (NGC 424, NGC 591, NGC 2273, NGC 3081, and NGC 4507), establishing that these objects are type 1 Seyferts obscured by dense circumnuclear material. The galaxies are part of a distance-limited sample of 31 Seyfert 2s, for which spectropolarimetric observations are now complete. Combined with published reports, our results indicate that at least 11 of the galaxies in this sample, or $\geq 35\%$, possess hidden broad-line regions. This represents the first reliable estimate of the frequency of polarized broad emission lines in type 2 Seyferts, which has important implications for the general applicability of Seyfert unification models.

Subject headings: galaxies: active — galaxies: individual (NGC 424, NGC 591, NGC 2273, NGC 3081, NGC 4507) — galaxies: Seyfert — polarization

1. Introduction

Seyfert galaxies have traditionally been classified into two spectroscopic groups based on the presence (type 1) or absence (type 2) of permitted optical emission lines that are broader than their forbidden lines. The discovery of polarized broad lines in NGC 1068 (Antonucci & Miller 1985) and a handful of other type 2 Seyfert galaxies (Miller & Goodrich 1990; Tran, Miller, & Kay 1992; Tran 1995a; Young et al. 1996; Heisler, Lumsden, & Bailey 1997; Kay & Moran 1998) has therefore had significant impact on our understanding of the relationship between the two types of objects and, more generally, of the parsec-scale geometry of Seyfert nuclei. The polarization, interpreted to be due to nuclear light that is scattered into our line of sight, establishes that some Seyfert 2s harbor normal Seyfert 1 nuclei whose innermost regions are obscured from our direct view, presumably by dense circumnuclear material. This material may be present in type 1 Seyferts as well, but oriented such that it does not lie between us and the central engine of the active nucleus.

¹Chandra Fellow.

²Department of Astronomy, University of California, Berkeley, CA 94720-3411.

³Harvard-Smithsonian Center for Astrophysics, 60 Garden Street, Cambridge, MA 02138.

⁴Department of Physics and Astronomy, Barnard College, Columbia University, New York, NY 10027.

⁵Visiting Astronomer, Cerro Tololo Inter-American Observatory. CTIO is operated by AURA, Inc., under contract with the National Science Foundation.

One hindrance to the extrapolation of this unified picture to *all* Seyfert galaxies is the fact that direct evidence for obscured type 1 nuclei in type 2 objects has been limited to relatively few examples. Thus, to explore the nature of the activity in Seyfert 2 galaxies as a class, we have initiated a multiwavelength survey of a distance-limited sample of 31 objects, beginning with spectropolarimetric observations. In this *Letter*, we announce the discovery of “new” hidden broad-line regions in five Seyfert 2 galaxies from this sample; full results of our survey will be presented in a forthcoming paper (Kay et al. 2000). Because of the unbiased nature of the survey, which is now complete, we are able to make the first reliable assessment of the frequency of polarized broad emission lines in type 2 Seyferts.

2. Observations and Results

Our survey is based on the distance-limited sample of Ulvestad & Wilson (1989, hereafter UW89), which, at the time of its definition, comprised all known Seyfert galaxies (31 of type 2)⁶ with recession velocities $cz < 4600 \text{ km s}^{-1}$ and declinations $\delta > -45^\circ$. Although some additional Seyfert 2s have been identified within the UW89 distance limit over the past decade, most of them are inconspicuous, low-luminosity objects that were classified either by inference, as in the instance of NGC 3147 (Moran, Halpern, & Helfand 1994; Ptak et al. 1996), or after careful starlight template subtraction of the optical spectrum (Ho, Filippenko, & Sargent 1997). Thus, the UW89 sample represents a reasonably complete, distance-limited set of *classical* Seyfert 2s. The sample was originally used to examine the radio properties of Seyfert galaxies; radio results obtained for the magnitude-limited CfA sample of Seyferts (Kukula et al. 1995) are consistent with those of UW89, suggesting that the UW89 sample is free of significant selection biases.

The spectropolarimetry component of our Seyfert 2 survey is now complete. Observations of the five UW89 objects in which we have discovered polarized broad emission lines were carried out at the Keck-II 10 m telescope on (UT) 7 March 1998 and 6 January 1999, and at the CTIO 4 m telescope on 23 June 1998 and 20 June 1999. Table 1 lists these galaxies and their recession velocities, as well as the observatory and exposure times employed. Reduction and analysis of the data were performed as described by Barth, Filippenko, & Moran (1999) and Kay et al. (1999). The observed continuum polarization P_{obs} and linear polarization position angle (P.A.) θ of each object in the 5400–5600 Å (rest) wavelength range are also listed in Table 1. For all of the galaxies, θ remains approximately constant across the Balmer-line profiles.

Spectropolarimetric results are shown for all five galaxies in Figures 1–5. As indicated in the upper panel in each of the Figures, only narrow emission lines are present in the total-flux spectra of the objects. The polarization spectra (middle panel) of the galaxies all display similar

⁶UW89 considered 35 galaxies to be Seyfert 2s (see their Table 6), but recent spectroscopy has revealed that three of them (MS 0942.8+0950, NGC 1365, and Mrk 1126) are actually intermediate type 1 objects. Over the course of our survey, we have found that one other (Mrk 745) is a high-ionization H II galaxy rather than a Seyfert.

characteristics: low but nonzero continuum polarization, depressions in polarization at the locations of strong narrow emission lines (e.g., [O III] $\lambda\lambda 4959, 5007$), and increases in polarization in the wings of the H α and (in most cases) H β lines. The product of the polarization and total-flux spectra (bottom panel) reveals broad permitted emission lines in the polarized flux of each galaxy.

NGC 424. As Figure 1 indicates, there is a distinct increase in the polarization of this object near H α . The H α line in polarized flux is very broad, with a full-width near zero-intensity (FWZI) of at least 12,000 km s $^{-1}$, which is much broader than the FWZI of the narrow [N II] + H α blend in the total-flux spectrum shown in the upper panel of Figure 1. There is clearly a broad component of H β in the polarized flux spectrum as well.

NGC 591 (Mrk 1157). Enhancements in polarization near H α and H β are subtle in this object, but as Figure 2 shows, both lines exhibit broad components in polarized flux. The FWZI of the broad H α line is ~ 4000 km s $^{-1}$. Following Barth et al. (1999), we have assessed the significance of our detection of H α polarization by comparing the mean values of the Stokes parameters Q and U across the broad H α profile to those in adjacent line-free regions. We find that Q and U across H α deviate from the continuum levels by 1.9 σ and 9.5 σ , respectively. Polarized broad H α emission was not detected by Miller & Goodrich (1990) in shallower observations with the Lick 3 m telescope.

NGC 2273 (Mrk 620). This is another weakly polarized object, but there is an obvious bump at H α in the polarization spectrum (Fig. 3), which is more prominent in polarized flux. The FWZI of the broad H α line is ~ 5000 km s $^{-1}$. The significance of our detection of a broad H α feature is 8.0 σ in Stokes Q , and 2.3 σ in Stokes U .

NGC 3081. Very strong enhancements of the polarization near both H α and H β are observed in this object (Fig. 4), yielding a spectacular type 1 spectrum in polarized light. The broad component of H α has FWZI ≈ 7000 km s $^{-1}$. It appears that the He I $\lambda 5876$ line is polarized as well.

NGC 4507. Similar to NGC 3081, this galaxy exhibits significant polarization enhancements near the Balmer lines, particularly H α (Fig. 5). A bump near He I $\lambda 5876$ also appears in the polarization spectrum. In polarized flux, the broad H α line is strong and asymmetric, with FWZI $\approx 10,000$ km s $^{-1}$.

Many Seyfert 2s with polarized broad emission lines have morphologically “linear” radio sources in their nuclei. In such cases, the major axis of the radio emission is often orthogonal to the polarization position angle θ (Antonucci 1983, 1993). Only two objects studied here, NGC 591 and NGC 2273, have linear radio sources; in the others, the emission is unresolved or only marginally resolved on $\sim 1''$ scales (Ulvestad & Wilson 1984, 1989; Morganti et al. 1999). For NGC 591, the radio axis lies along P.A. = 153 $^\circ$, which is almost perpendicular to θ (Table 1). The radio axis of NGC 2273 lies along P.A. = 90 $^\circ$, whereas $\theta = 25^\circ$. Because of the weak overall polarization of this object, an interstellar component of polarization, which we have not corrected for, could be affecting both P_{obs} and θ .

Unpolarized starlight from the host galaxies contributes a major, if not dominant, fraction of the observed continuum fluxes, diminishing the polarization of the nuclear emission. Thus, following the methods of Tran (1995a), we have attempted to correct for the effects of starlight dilution to obtain a better measurement of the true level of continuum polarization in each object. This involves decomposition of the observed spectrum into stellar and nonstellar components using spectra of elliptical galaxies and spiral galaxy bulges free of emission lines as starlight templates. Best results for our galaxies were generally obtained with spectra of NGC 224 (M31) or NGC 7457 as templates (a full description of the analysis will be presented by Kay et al. 2000). The derived fractions of galactic starlight F_g present in our Seyfert 2 spectra are listed in Table 1. Corrected values of the continuum polarization P_{cor} [$= P_{\text{obs}}/(1 - F_g)$] are also listed in the Table.

3. Location and Geometry of the Obscuring Medium

The currently popular picture for the parsec-scale geometry of Seyfert nuclei, originally proposed by Antonucci & Miller (1985), contends that the broad-line region (BLR) and optical/UV continuum source are surrounded by dense material that has a roughly toroidal geometry; the orientation of this torus to our line of sight thus determines the optical spectroscopic classification of a given Seyfert galaxy. In some type 2 Seyferts, where the torus is presumably edge-on, free electrons or dust grains located above the opening of the torus scatter nonstellar continuum and broad-line photons into our line of sight. Because the scattered emission is polarized, spectropolarimetric observations can provide a perisopic view of the innermost regions of these objects. Unfortunately, selection effects have often confounded studies intended to test the general applicability of the torus model (Antonucci 1993), and it has been unclear what fraction of the Seyfert 2 population it describes. In fact, a recent imaging survey by Malkan, Gorjian, & Tam (1998) has revealed that type 2 Seyferts are more likely than Seyfert 1s to have dust lanes and patches close (in projection) to the nucleus, suggesting that interstellar dust hundreds of parsecs from the active nucleus, rather than a parsec-scale circumnuclear torus, may be the main source of extinction in the majority of Seyfert 2 galaxies.

Spectropolarimetry provides independent evidence regarding the location and geometry of the obscuring medium in Seyfert 2 galaxies. As Figures 1–5 and the results of Tran (1995b) indicate, the narrow emission lines of objects with hidden BLRs are less polarized than the continuum and broad Balmer lines. Thus, most of the scattering takes place interior to the narrow-line region, which, for reasonable values of the black-hole mass ($10^8 M_{\odot}$) and narrow emission-line velocity widths (500 km s^{-1} FWHM), has an inner dimension of order 10 pc. For us to detect polarized emission, the projected size of the obscuring material must be comparable to or smaller than the size of the scattering region, implying that the obscuration occurs close to the black hole. In principle, significant polarization could result from scattering of an isotropic radiation field by a patchy medium, but the relationship between the polarization and radio-source position angles in Seyfert 2s would then have to be a coincidence. The alternative is that the radiation field

somehow becomes anisotropic prior to scattering (Antonucci 1984). In this scenario, the high (5–16%) starlight-corrected polarizations of NGC 3081, NGC 4507, and several galaxies in the Tran (1995a,b) study are possible if the obscuring material covers much of the nucleus in the equatorial plane. We conclude, therefore, that the material primarily responsible for the obscuration of those Seyfert 2s with hidden BLRs and high intrinsic polarizations is located close to the black hole and, qualitatively, is cylindrically symmetric—a torus, for all practical purposes. (Note that a highly warped, thin accretion disk might also be capable of providing the necessary scattering geometry; see Phinney 1989.) There is no reason to suspect that the hidden-BLR Seyfert 2s lacking high starlight-corrected polarizations are fundamentally different. As discussed by Miller & Goodrich (1990), the scattering medium may be located within the mouth of the torus, rather than above it; polarized emission would then only be detectable in objects where the torus is tipped toward us, and in such cases, polarization levels would be modest. Infrared and hard X-ray observations appear to support this picture (Heisler et al. 1997; Risaliti et al. 2000).

4. Frequency of Polarized Broad Lines in Type 2 Seyferts

While previous spectropolarimetric observations have demonstrated that some type 2 Seyferts are type 1 objects obscured by dense circumnuclear material, it has been unclear what fraction of Seyfert 2s can be described this way. A determination of the frequency of polarized broad emission lines in Seyfert 2s, now possible with the completion of our survey of the UW89 sample, provides an important lower limit on this fraction.

Five of the 31 galaxies in the UW89 sample were known to possess hidden BLRs prior to the start of our survey: NGC 1068 (Antonucci & Miller 1985), Mrk 3 and Mrk 348 (Miller & Goodrich 1990), NGC 4388 (Shields & Filippenko 1988; Young et al. 1996), and IC 3639 (Heisler et al. 1997). As discussed by Kay et al. (2000), we have confirmed the presence of hidden BLRs in these last two objects. Combined with our discovery of polarized broad emission lines in NGC 788 (Kay & Moran 1998), the five detections presented here in NGC 424, NGC 591, NGC 2273, NGC 3081, and NGC 4507 have more than doubled the number of known hidden BLRs in this sample, bringing the total to 11. Higher quality observations could, of course, increase this number. Thus, at least 35% of nearby classical Seyfert 2s have polarized broad permitted emission lines, indicating that they are obscured primarily by material located a few parsecs from the nucleus, rather than by large-scale foreground dust lanes. The remainder, however, may be obscured mainly by interstellar matter, as suggested by Malkan et al. (1998), or they may simply lack BLRs.

Hard X-ray observations of Seyfert 2 galaxies complement spectropolarimetric data by providing a measure of the amount of absorbing material present. For example, recent hard X-ray observations have shown that $\sim 50\%$ of Seyfert 2s (from a different sample) have absorption column densities too high ($N_{\text{H}} > 10^{24} \text{ atoms cm}^{-2}$) to be associated with interstellar dust features (Risaliti, Maiolino, & Salvati 1999). This is consistent with the lower limit of 35% we have derived for the fraction of Seyfert 2s that are obscured by circumnuclear tori. Nearly all of the Seyfert 2s

in the UW89 sample have been observed in the hard X-ray band, and in a future paper we will combine those observations with our spectropolarimetric results to explore further the nature of the obscuring material in type 2 Seyfert galaxies.

We are very grateful to Michael Eracleous for assistance with the starlight fraction measurements, and to A. M. Magalhães for supplying the polarimetry optics used at CTIO. The W. M. Keck Observatory is operated as a scientific partnership among the California Institute of Technology, the University of California, and NASA, and was made possible by the generous financial support of the W. M. Keck Foundation. E. C. M. is supported by NASA through Chandra Fellowship grant PF8-10004 awarded by the Chandra X-ray Center, which is operated by the Smithsonian Astrophysical Observatory for NASA under contract NAS 8-39073. The work of A. J. B. is supported by a postdoctoral fellowship from the Harvard-Smithsonian Center for Astrophysics. L. E. K. acknowledges the support of the NSF through CAREER grant AST-9501835. We also acknowledge NASA grant NAG 5-3556.

REFERENCES

Antonucci, R. R. J. 1983, *Nature*, 303, 158
———. 1984, *ApJ*, 278, 499
———. 1993, *ARA&A*, 31, 473
Antonucci, R. R. J., & Miller, J. S. 1985, *ApJ*, 297, 621
Barth, A. J., Filippenko, A. V., & Moran, E. C. 1999, *ApJ*, 525, 673
Heisler, C. A., Lumsden, S. L., & Bailey, J. A. 1997, *Nature*, 385, 700
Ho, L. C., Filippenko, A. V., & Sargent, W. L. W. 1997, *ApJS*, 112, 315
Kay, L. E., Magalhães, A. M., Elizalde, F., & Rodrigues, C. 1999, *ApJ*, 518, 219
Kay, L. E., & Moran, E. C. 1998, *PASP*, 110, 1003
Kay, L. E., & Moran, E. C., Barth, A. J., & Filippenko, A. V. 2000, in preparation
Malkan, M. A., Gorjian, V., & Tam, R. 1998, *ApJS*, 117, 25
Miller, J. S., & Goodrich, R. W. 1990, *ApJ*, 355, 456
Miller, J. S., Robinson, L. B., & Goodrich, R. W. 1988, in *Instrumentation for Ground-Based Astronomy*, ed. L. B. Robinson (New York: Springer), 157
Moran, E. C., Halpern, J. P., & Helfand, D. J. 1994, *ApJ*, 433, L65

Morganti, R., Tsvetanov, Z. I., Gallimore, J., & Allen, M. G. 1999, *A&AS*, 137, 457

Phinney, E. S. 1989, in *Theory of Accretion Disks*, eds. W. Duschl, F. Meyer, & J. Frank (Dordrecht: Kluwer), 457

Ptak, A., Yaqoob, T., Serlemitsos, P. J., Kunieda, H., & Terashima, Y. 1996, *ApJ*, 459, 542

Risaliti, G., Gilli, R., Maiolino, R., & Salvati, M. 2000, *A&A*, 357, 13

Risaliti, G., Maiolino, R., & Salvati, M. 1999, *ApJ*, 522, 157

Shields, J. C., & Filippenko, A. V. 1988, *ApJ*, 332, L55

Tran, H. D. 1995a, *ApJ*, 440, 565

———. 1995b, *ApJ*, 440, 578

Tran, H. D., Miller, J. S., & Kay, L. E. 1992, *ApJ*, 397, 452

Ulvestad, J. S., & Wilson, A. S. 1984, *ApJ*, 285, 439

———. 1989, *ApJ*, 343, 659 (UW89)

Young, S., Hough, J. H., Efstathiou, A., Wills, B. J., Bailey, J. A., Ward, M. J., & Axon, D. J. 1996, *MNRAS*, 281, 1206

Table 1. Spectropolarimetric Observations and Results

Galaxy	cz (km s $^{-1}$)	Obs.	Exp. (s)	P_{obs} (%)	θ (deg)	F_g	P_{cor} (%)
NGC 424	3496	CTIO	3600	2.31 ± 0.03	43 ± 1	0.45	4.2
NGC 591	4547	Keck	1200	0.53 ± 0.07	70 ± 4	0.52	1.1
NGC 2273	1871	Keck	1200	0.26 ± 0.07	25 ± 7	0.80	1.3
NGC 3081	2385	Keck	1200	1.43 ± 0.07	79 ± 1	0.89	13.0
NGC 4507	3538	Keck	800	0.79 ± 0.05	37 ± 2	0.87	6.1

Note. — P_{obs} , θ , F_g , and P_{cor} are continuum values measured in the 5400–5600 Å (rest) wavelength range.

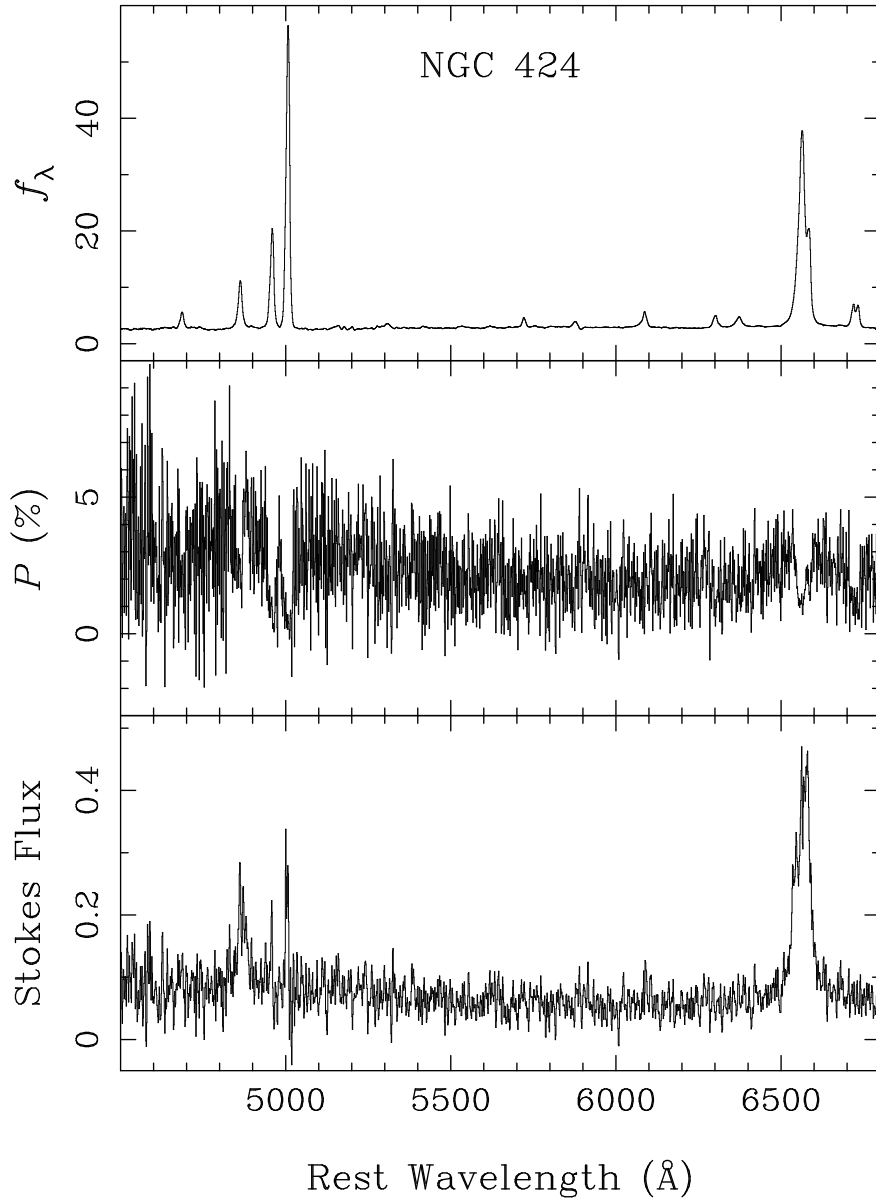


Fig. 1.— Spectropolarimetry of NGC 424. Corrections for interstellar polarization and starlight dilution have not been applied. Only narrow emission lines are present in the total-flux spectrum of the galaxy (*top panel*), which has units of 10^{-15} erg $\text{cm}^{-2} \text{s}^{-1} \text{\AA}^{-1}$. The polarization spectrum (*middle panel*) shows that the polarization is enhanced in the wings of the H α and H β lines. (The polarization P shown here is actually the “rotated Stokes parameter”; see Miller, Robinson, & Goodrich 1988.) The polarized flux, or “Stokes flux” (*bottom panel*) is the product of the total-flux and polarization spectra. Broad components of both H α (FWZI $\approx 12,000$ km s^{-1}) and H β are evident in polarized flux.

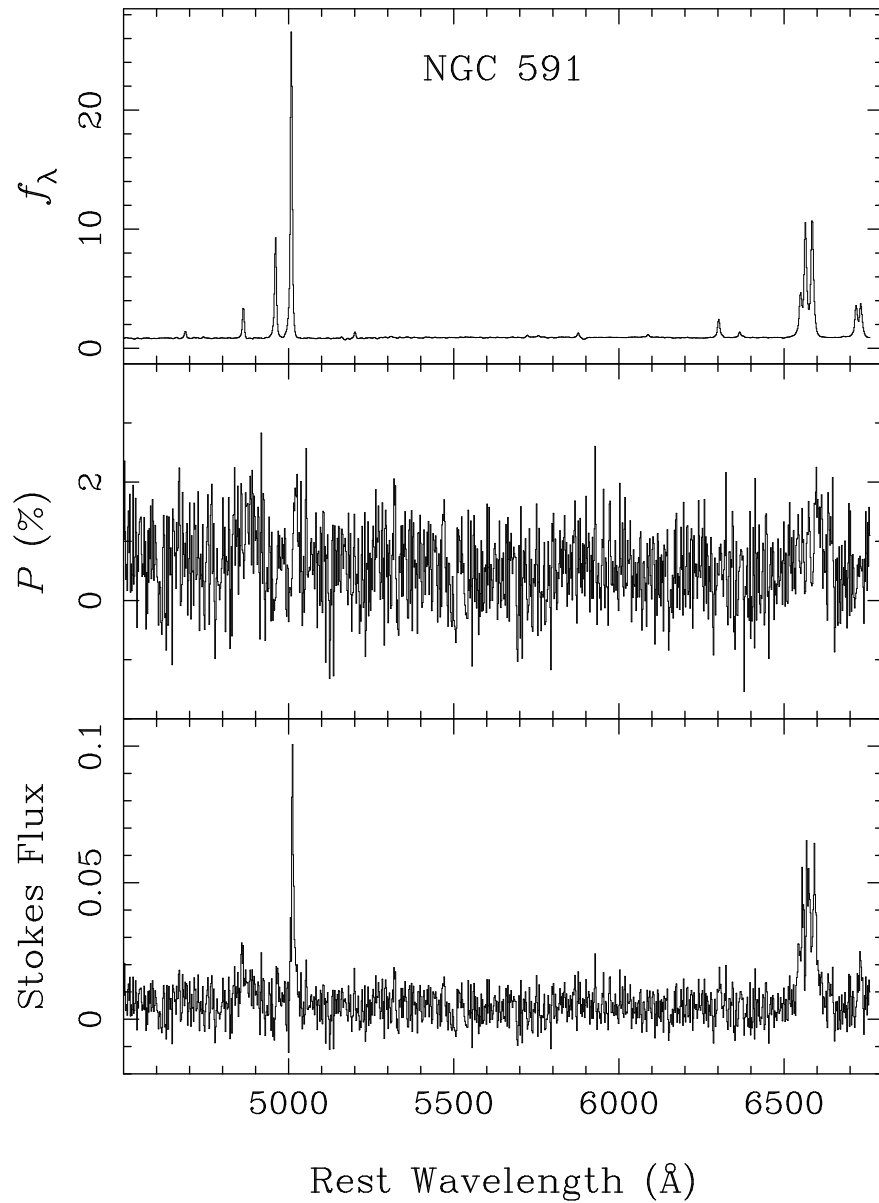


Fig. 2.— Spectropolarimetry of NGC 591.

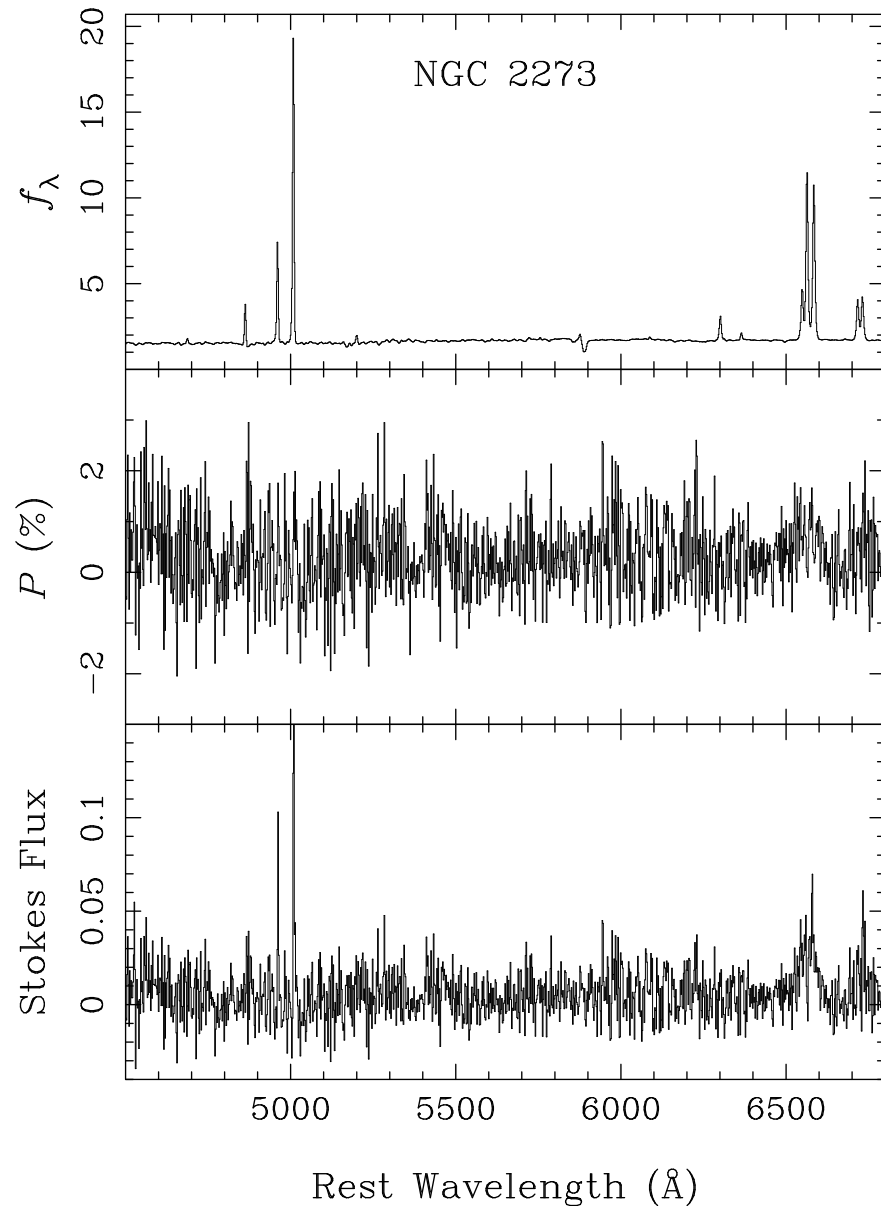


Fig. 3.— Spectropolarimetry of NGC 2273.

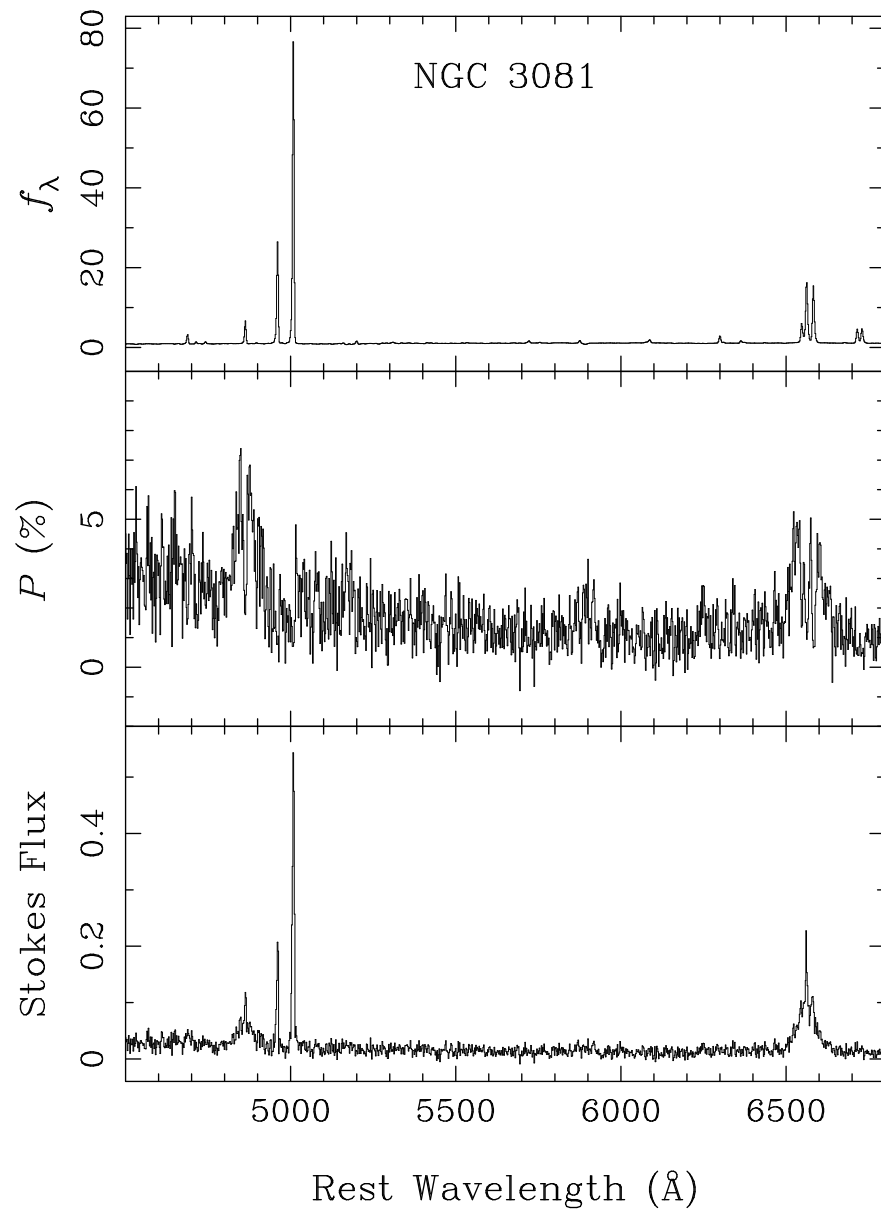


Fig. 4.— Spectropolarimetry of NGC 3081.

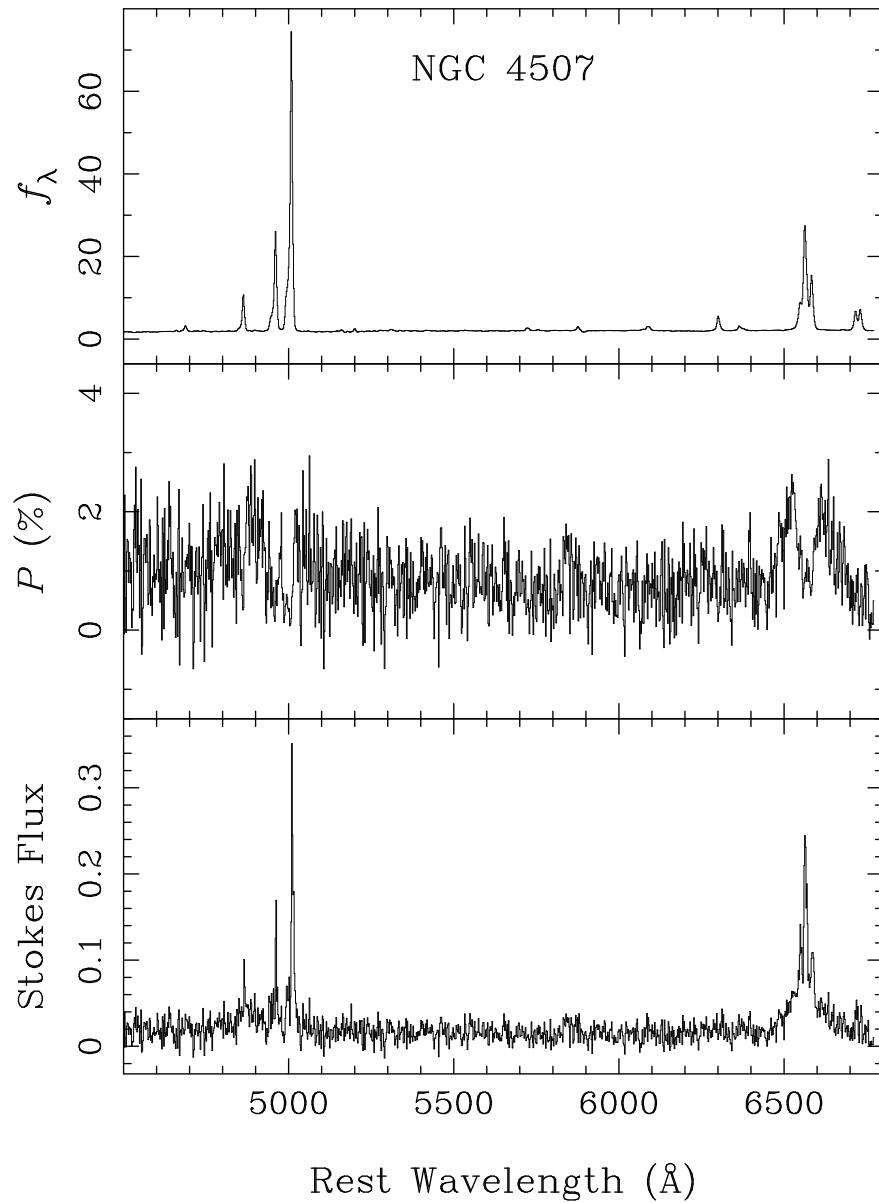


Fig. 5.— Spectropolarimetry of NGC 4507.